5

Inner Shells

B. FRICKE

1. Introduction

Interest in the physics of atomic inner shells is currently undergoing a renaissance after lying nearly dormant for some forty years. In the early days of quantum mechanics many basic problems were formulated in principle but had to be set aside as intractable in practice. Many of these can now be solved with modern experimental and theoretical techniques. From the experimental point of view the rapidly increasing interest in inner shells since the late 60s is the result of the availability of highly ionized heavy atoms with energies sufficient to reach the domain of inner-shells at a great number of small- and medium-sized accelerators. The experimental results together with the rapid development of faster and larger computers has stimulated this field from the theoretical point of view. The accuracy of the best Hartree–Fock calculations available nowadays already allows a quasiexperimental determination of the quantum electrodynamical contributions for the inner shells of high-Z atoms. This method as well as the results for the binding energies of inner shells for low Z, large Z, and superheavy Z (larger than 137) will be discussed in the first part of this chapter. In the second part the inner-shell vacancy production mechanisms such as Coulomb ionization and molecular excitation will be discussed very briefly. During the collision, combined atom or quasimolecular phenomena appear, which will be considered in the last part of this chapter.

B. FRICKE • Gesamthochschule Kassel, D 35 Kassel, Germany.

2. Binding Energies of Inner Electrons

2.1. Method of Calculation

How well do the experimental binding energies of atomic electrons compare with theoretical calculations? This is one of the basic questions in atomic physics. The method of calculation of binding energies from a theoretical point of view was given by Hartree and Fock[1] in the late 1920s.

2.1.1. Hartree–Fock Calculations

The so-called Hartree–Fock method is the basis of all good atomic calculations. This method with the various assumptions and approximations used nowadays is discussed in this book in Chapter 1. Only the nonrelativistic methods are reviewed there. Because we are interested here in the inner electrons, we must include the relativistic methods. As we shall see, even for neon ($Z = 10$) relativistic effects cannot be neglected and, for larger-Z atoms, nonrelativistic attempts to describe the atom are absolutely wrong. The difference between the nonrelativistic and the relativistic description first given by Dirac[2] is in the different kinetic energy operator. The relativistic Hamiltonian for the many-electron system may be expressed as

$$\mathbf{H} = \sum_{i}^{\substack{\text{all } N \\ \text{electrons}}} \left[-ic\boldsymbol{\alpha}_i \boldsymbol{\nabla}_i + \boldsymbol{\beta}_i c^2 - \frac{Z}{r_i} \right] + \sum_{i<j} \frac{1}{r_{ij}} \tag{1}$$

where $\boldsymbol{\alpha}$ and $\boldsymbol{\beta}$ are the Dirac 4×4 matrices

$$\boldsymbol{\alpha} = \begin{pmatrix} 0 & \boldsymbol{\sigma} \\ -\boldsymbol{\sigma} & 0 \end{pmatrix}, \qquad \boldsymbol{\beta} = \begin{pmatrix} \mathbf{1} & 0 \\ 0 & -\mathbf{1} \end{pmatrix}$$

with $\boldsymbol{\sigma}$ the Pauli matrices and $\mathbf{1}$ the unit matrix.

Using this relativistic Hamiltonian the resulting Hartree–Fock equations for the radial functions, where μ and ν are indices running over all occupied levels, take the following form:

$$\frac{dP_\mu}{dr} + \frac{k_\mu}{r} P_\mu = \left[2c + \frac{1}{c}(\varepsilon_\mu - V_\mu) \right] Q_\mu + W_Q + \frac{1}{c} \sum_{\mu \neq \nu}^{N} \varepsilon_{\mu\nu} Q_\nu \tag{2}$$

$$-\frac{dQ_\mu}{dr} + \frac{k_\mu}{r} Q_\mu = \frac{1}{c}(\varepsilon_\mu - V_\mu) P_\mu + W_P + \frac{1}{c} \sum_{\mu \neq \nu}^{N} \varepsilon_{\mu\nu} P_\nu \tag{3}$$

with

$$V_\mu = \frac{1}{r}\left[-Z + \sum_\nu \sum_k q_\nu A_k^E(\mu, \nu) Y_k(\nu, \nu)\right] \tag{4}$$

$$W_{P \text{ or } Q} = \frac{1}{rc} \sum_\nu \sum_k q_\nu B_k^E(\mu, \nu) Y_k(\mu, \nu) P_\nu \text{ or } Q_\nu \tag{5}$$

$$Y_k(\mu, \nu) = r \int_0^\infty [P_\mu(s) P_\nu(s) + Q_\mu(s) Q_\nu(s)] U_k(r, s)\, ds \tag{6}$$

$$U_k(r, s) = \begin{cases} r^k/s^{k+1} & \text{if } r \leqslant s \\ s^k/r^{k+1} & \text{if } r > s \end{cases}$$

P and Q are the large and small components of the wave functions, respectively; A^E and B^E are angular coefficients. For details of the relativistic Hartree–Fock method see Grant.[3] The relativistic Hartree–Fock equations (2)–(6) can easily be compared with the nonrelativistic expression in Chapter 1 of this book.

The main difference is that we now have a coupled system of $2N$ differential equations of first order for the large and the small components P and Q of the wave functions compared to the N coupled equations of second order in the nonrelativistic case.

These coupled differential equations have to be solved by iteration to self-consistency. As a result we get a value for the total energy. The binding energies E_{bind} of the electrons are given by the difference of the total energies E_T of the whole atom before and after the ionization:

$$E_{\text{bind}} = E_T(\text{atom}) - E_T(\text{ion})$$

If we use the results from such relativistic Hartree–Fock (or Dirac–Fock) calculations and compare them with experimental binding energies of inner electrons in very heavy atoms, we still find a discrepancy of the order of 1%. Approximations to this Dirac–Fock method such as Dirac–Slater or Dirac–Fock–Slater calculations (see Ref. 3) may yield better agreement with experimental results but may not be taken as better methods because they have an adjustable parameter and are, therefore, not fully *ab initio* methods.

2.1.2. Additional Effects (Magnetic, Retardation, QED)

At this level of sophistication all additional effects not taken into account so far have to be included. These are the magnetic effects, the influence of retardation in the interaction of the electrons, the quantum electrodynamic effects—vacuum polarization and self-energy (or vacuum fluctuation), and the correlation energy.

Although the total effect of the correlation energy may be large, the net effect can be neglected for the inner electrons in very heavy atoms because we have to deal here with differences of the same magnitude.[4]

The Hamiltonians of all four remaining additional effects are known only as perturbations, so their contribution can be computed consistently in a perturbation calculation only. The magnetic energy and the retardation[5] are given by the well-known Breit Hamiltonian

$$H_B = H_{\text{mag}} + H_{\text{retard}} = -\frac{1}{2}\left[\frac{\boldsymbol{\alpha}_i \cdot \boldsymbol{\alpha}_j}{r_{ij}} + \frac{(\boldsymbol{\alpha}_i r_{ij}) \cdot (\boldsymbol{\alpha}_j r_{ij})}{(r_{ij})^3}\right] \tag{7}$$

The vacuum polarization to first order in $(Z\alpha)$ can be expressed[6] by a local potential

$$V_{\text{V.P.}} = \frac{2\alpha e^2}{3\pi} \int \frac{\rho(\mathbf{r}')}{|\mathbf{r}-\mathbf{r}'|} Z_0(|\mathbf{r}-\mathbf{r}'|)\, dJ' \tag{8}$$

with

$$Z_n(|\mathbf{r}|) = \int_1^\infty \exp\left(-\frac{2}{\lambda_e}|\mathbf{r}|\xi\right)\left(1+\frac{1}{2\xi^2}\right)\frac{(\xi^2-1)^{1/2}}{\xi^2} \cdot \frac{1}{\xi^n}\, d\xi \tag{9}$$

and $\lambda_e = 386$ fm and $\rho(\mathbf{r})$ is the nuclear charge density; the self-energy part, on the other hand, cannot be given by a simple expression. For these two QED corrections we also refer to Chapter 4 in this book on the Lamb shift. For large Z the vacuum fluctuation can be calculated according to the theory of Brown *et al.*[7] and the new calculations of Desiderio *et al.*[8] and Mohr.[9]

2.2. *Results and Comparison with Experiments*

2.2.1. *Low-Z, Highly Ionized Atoms*

A large number of excellent measurements of the spectra of highly ionized and excited atoms have been performed during recent years. For details see Chapter 17 of this work and Refs. 10 and 11. Because of the great complexity of the spectra many groups have focused their interest on highly ionized few-electron systems,[12] where it is still possible to handle the problem from the theoretical point of view. For example in Figure 1 part of the beam-foil excited Auger electron spectrum[13] of Ne on C is shown measured in coincidence with the outgoing projectile having the well-defined charge state 8^+. At the top of this figure the calculated transition energies are given; they fit the experimental data very well. In these calculations the even better and much more complicated multi-configuration Dirac–Fock method was used instead of the Dirac–Fock treatment discussed above.

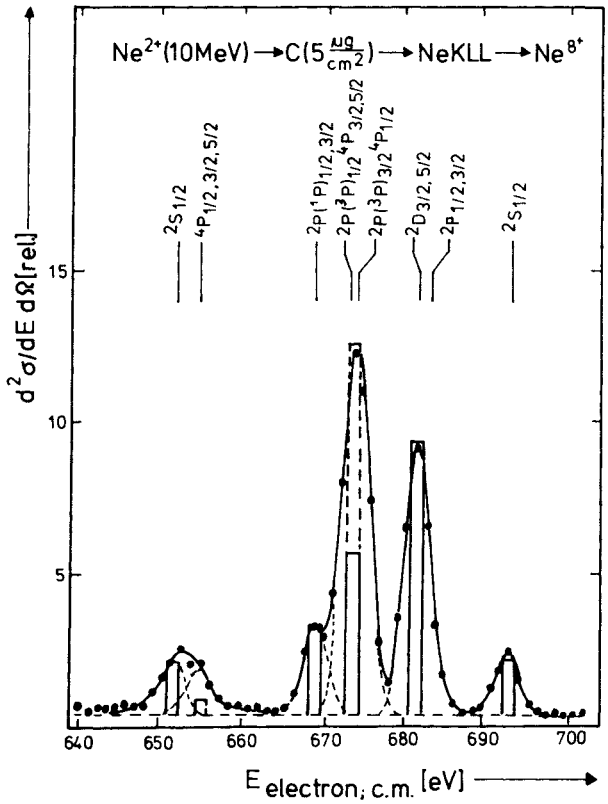

Figure 1. The KLL Auger spectrum of neon measured in coincidence with Ne^{8+} projectiles after bombarding a carbon foil. In the upper half comparison with levels from multiconfiguration Dirac–Fock calculations are given.

If we compare these results with the analogous nonrelativistic calculations we find a large shift of the two lines on the extreme right and extreme left of the spectrum in Figure 1. These two lines have large contributions from the $2s$ electron level, which is strongly influenced by the relativistic effects. This one example shows that only a full relativistic analysis of the spectra of highly ionized atoms with low Z leads to good agreement and thus relativistic effects have to be introduced even in this part of the periodic system.

2.2.2. Heavy Atoms with Inner Shell Vacancies

A comparison of theoretical and experimental binding energies of inner-shell electrons in very heavy atoms is very important for several

Table 1. Comparison of Experimental Binding Energies (in keV) of Inner Electrons in Fermium ($Z = 100$) with Theoretical Dirac–Fock Calculations Plus All Known Additional Corrections

Source	Level					
	$1s$	$2s$	$2p_{1/2}$	$2p_{3/2}$	$3s$	$3p_{1/2}$
Electric	−142.929	−27.734	−26.791	−20.947	−7.250	−6.815
Magnetic	+0.715	+0.091	+0.153	+0.092	+0.019	+0.033
Retardation	−0.041	−0.008	−0.013	−0.011	−0.001	−0.003
Vacuum fluctuation	+0.457	+0.096	+0.009	−0.003	+0.025	+0.003
Vacuum polarization	−0.155	−0.026	−0.004	+0.000	−0.006	−0.001
Theoretical total	−141.953(26)	−27.581(20)	−26.646(10)	−20.869(10)	−7.213(15)	−6.783(4)
Experimental value[a]	−141.963(13)	−27.573(8)	−26.664(7)	−20.868(7)	−7.200(9)	−6.779(7)

[a] Reference 16.

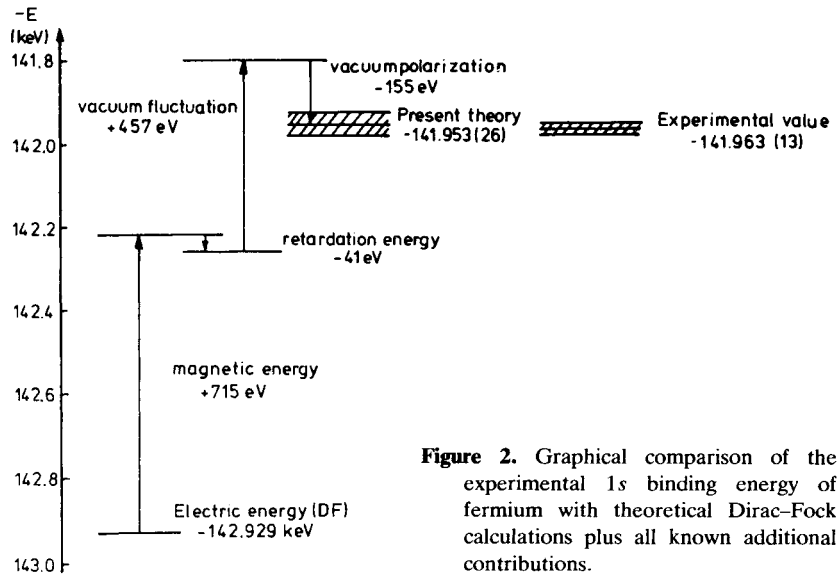

Figure 2. Graphical comparison of the experimental $1s$ binding energy of fermium with theoretical Dirac–Fock calculations plus all known additional contributions.

reasons. The first question is: "How good are the Dirac–Fock calculations?" This question is nontrivial because the Dirac equation itself is, in principle, a single-partial equation and the inclusion of more electrons cannot be justified from first principles. The second question is: "How large are the additional effects discussed in Section 2.1.2?" The third question is: "Do we need to take into account further effects such as nonlinear electrodynamic contributions, which were discussed by Greiner *et al.*[14]?"

Because all these effects, and thus the possible discrepancies, strongly increase with Z, the best way to answer these questions is to examine the highest element yet measured. In Table 1 a comparison[15] is given for the innermost electrons of fermium ($Z = 100$) measured by Porter *et al.*[16] In the calculated electric energies as well as the magnetic energies the relaxation effect due to the rearrangement from the atom to the ion is included.The error in the theoretical calculation still is of the order of 20 eV because of the uncertainty in the calculation of the self-energy. Table 1 definitely shows that the agreement for all the inner levels is within the error bars. This excellent agreement is also shown for the $1s$ level in Figure 2. A similar comparison of x-ray lines from plutonium and thorium[17] also leads to astonishingly good results.

This shows that the answers to our questions are as follows. The Dirac–Fock approximation using the solution of the Dirac equation is an excellent method even as far as the element fermium ($Z = 100$). The

additional contributions are contained within the error limit of ±20 eV and we do not need to include, at this degree of accuracy, any additional effects. Since the experimental uncertainty is now within 1 eV,[17] however, much more work has to be done in the future from the theoretical point of view.

2.2.3. *Level Behavior for Atoms with $Z > 137$*

Bearing in mind the results in Table 1, which show an excellent agreement between theory and experiment, we can at least be relatively sure that theoretical calculations performed for even higher Z will be realistic approximations.

A magic limit is $Z = 137$ because at this point the solution of the Dirac equation for the $1s$ level of a hydrogenic atom, with a point nucleus, becomes imaginary. This limit can be circumvented if one uses an extended nucleus so that the divergency at $r = 0$ disappears. The resulting level behavior calculated from self-consistent Dirac–Slater calculations[18] is given in Figure 3.

Two interesting effects occur. The large spin–orbit splitting of levels such as the $2p_{1/2}$ and $2p_{3/2}$ or the $3p_{1/2}$ and $3p_{3/2}$ levels increases so

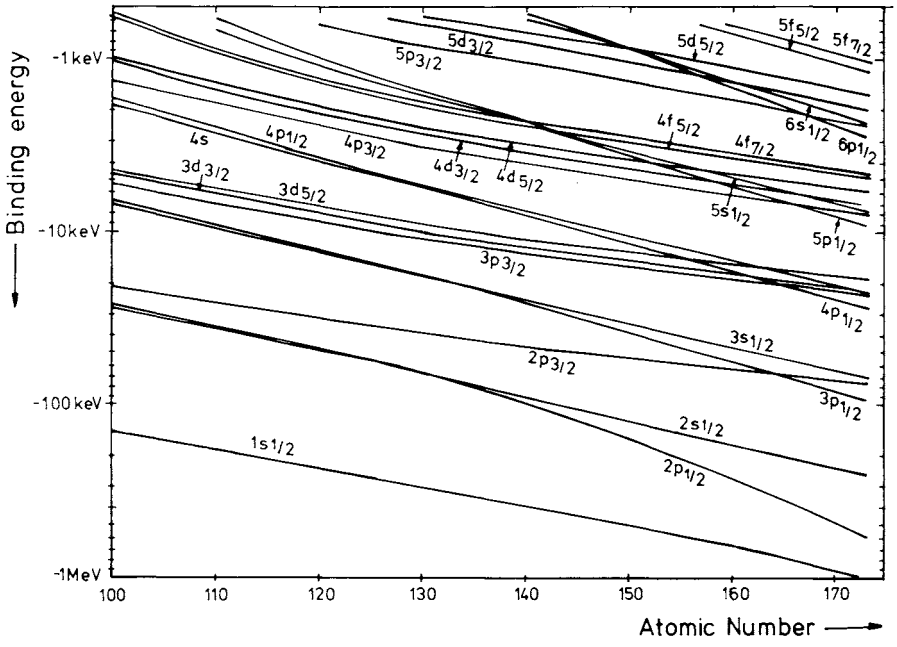

Figure 3. Inner atomic level for $100 < Z < 173$ from Dirac–Fock–Slater calculations.[18]

rapidly that their binding energy at $Z = 170$ differs already by factors of 6 and 4, respectively. The wave functions also change so much that the shielding for the $s_{1/2}$ electrons becomes much larger than the $p_{1/2}$ electrons having the same principal quantum number. As a result the $2p_{1/2}$ level becomes lower than the $2s_{1/2}$ level for Z above 130.

For even larger Z the ordering of the levels becomes very strange (see Figure 3). This will show up in the behavior of the outer levels and even in the predictions related to the chemistry of these elements.[19] The second, even more interesting result, is that at, or near, $Z = 173$ the $1s$ level dives into the negative continuum. For a long time it was not clear what would happen if such a bound level reached the negative continuum, until Müller *et al.*[20] found that this could well be interpreted in a way similar to a quasibound level in the positive continuum. They also predicted the creation of positrons when a hole is brought down into the negative continuum.

As we shall see in Section 4, this discussion of the level behavior is by no means academic since in the near future it will be possible to create quasi atoms with very large Z for a time of the order of 10^{-18} sec, by bombarding uranium with uranium, giving a united $Z = 184$. We refer to Section 4, where the united atom phenomena will be discussed briefly.

3. *Inner-Shell Vacancy Production Mechanisms*

Inner-shell excitation in atomic collisions has reached a refined stage within the past decade. Evidently, the relatively simplest collision system is that of a swift structureless point charge Z_1 of velocity v_1 penetrating a hydrogenlike atom (nuclear charge Z_2) while the electrons (orbital velocity u) are only slightly perturbed by the projectile. This condition is fulfilled,

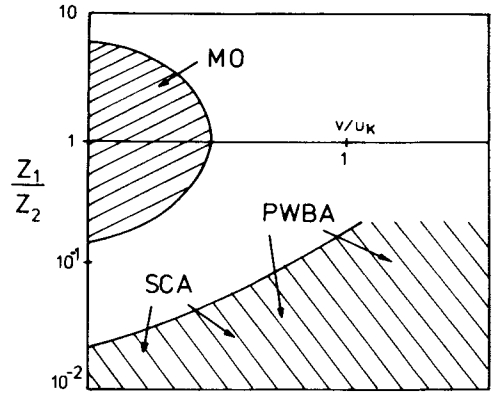

Figure 4. Regions of validity for various approximation schemes as a function of Z_1/Z_2 and collision velocity v (in units of the K-shell electron velocity u_K).

e.g., for inner shells in the case of $Z_1 \ll Z_2$ or $v_1 \gg u$. Such systems have been the subject of intense experimental and theoretical study,[21–23] which has resulted in a large body of data elucidating even the finer details of the interaction.[10,24] Generally, this region is termed "Coulomb excitation," indicating that excitation occurs mainly by direct Coulomb interaction between the projectile and the atomic electron. If the internal structure of the projectile and its influence on the target atom electrons cannot be neglected, particularly at low ion velocities $v_1 \ll u$ and comparable nuclear charges ($Z_1/Z_2 \approx 1$), the interaction tends to become more complex. This is the region of "molecular excitation," where excitation occurs by way of coupling between promoted levels in the quasimolecule formed during the collision.[25] These different regions are shown in Figure 4. The distinction between both regimes is helpful though somewhat arbitrary as it separates in a qualitative way regions in which different methods are applied.

3.1. Coulomb Ionization Processes

3.1.1. Plane-Wave Born Approximation (PWBA)

The first treatment by quantum mechanics of the ionization process was based on the Bethe–Born approximation.[26,21] In this approximation the incident charged particles are treated as plane waves, whereas the target electrons are described by hydrogenic wave functions. The interaction between the projectile and the electron is treated to first order. The PWBA formula for the differential cross section for Coulomb ejection of a target electron with final energy E_f is given by

$$\frac{d\sigma}{dE_f} = \frac{4\pi}{\hbar^2} Z_1^2 e^4 \frac{M_1}{E_1} \int_{q_0}^{\infty} \frac{dq}{q^3} I \tag{10}$$

with

$$I = \sum_f \left| \int e^{i\mathbf{q}\cdot\mathbf{r}} \psi_f^*(r) \psi_i(r)\, d\tau \right|^2 \tag{11}$$

Here $Z_1 e$, M_1, and E_1 are the charge, mass, and energy of the projectile. Further, $\hbar q$ denotes the momentum transfer with $\hbar q_0$ its minimum value. The quantities $\psi_{i,f}$ are the electron wavefunctions in the initial and final states, respectively. The summation in Eq. (11) is extended over all final electron states.

The condition for the Born approximation to be valid for the description of a collision between two particles with charges Z_1e and Z_2e, projectile and target, respectively, is given by the inequality

$$Z_1Z_2e^2 \ll \hbar v_1 \tag{12}$$

with v_1 being the relative velocity of the particles.[27] Nonrelativistic Coulomb wave functions have been used in Eq. (11) for the calculation of total ionization cross sections for various electron shells.[28,21] It appears that bombarding-energy dependences of the total Coulomb ionization cross sections are qualitatively described by PWBA calculations. This is well supported by experiments on K-shell Coulomb ionizations.[29] However, for K-shell ionizations, in particular, the agreement between experiment and nonrelativistic PWBA calculations is poor in the following two cases: (i) for very heavy target atoms, and (ii) at low projectile energies. For the heavy target atoms the PWBA Coulomb ionization cross sections are too small. Jamnik and Zupancic[30] have repeated the PWBA K-shell calculations with relativistic wave functions for the electrons. The relativistic increase of the electron density near the origin gives rise to an enlargement of the ionization cross sections, improving the agreement with experiment considerably. In the low-energy region, the inequality in Eq. (12) is no longer fulfilled. This manifests itself in PWBA cross sections that are too large compared to the experimental values. This fact was the impetus for the development of the semiclassical approximation model for atomic Coulomb excitation.

3.1.2. Binary Encounter Approximation (BEA)

Fairly recently Garcia[31] introduced the binary encounter approximation model (BEA) for the treatment of inner-shell ionizations by heavy charged particles based on the work of Gryzinski.[32] In this model the ionization process is considered as a classical impact between the projectile and a free target electron. The role ascribed to the rest of the atom is simply to provide the electron under consideration with a velocity distribution in its initial state. It should be noted that the BEA model may be looked upon as an example of the impulse approximation[33]; hence an agreement with the PWBA model at higher projectile energies is not surprising. From this rather simple but highly applicable model a scaling law is obtainable.[31] This law permits direct scaling of the total ionization cross sections for the respective inner electron shells for all target charges according to the binding energy of the electron shell in question. For the K-shell ionization the scaling law may be written in the following form:

$$E_K^2\sigma_K = g(E_1/E_K) \tag{13}$$

with g a general function to a good approximation, and the quantity E_K denoting the K-shell binding energy. For protons inducing K-shell ionization, in particular, the BEA model has yielded cross sections in very good agreement with experiment. At lower bombarding energies the agreement with measurement is not as good. However, approximate corrections for the nuclear repulsion of the projectile improves the agreement.[31]

Attempts have been made to improve the BEA model. In the original version of the model, relativistic effects on the velocity distribution and the mass of the target electron were not included. However, they have recently been considered by Hansen,[34] using rather complicated computations. Furthermore, McGuire[35] and McGuire and Omidvar[36] have established an impact parameter description of atomic K-shell ionization cross sections within the frame of the BEA picture, presumably inspired by the semiclassical approximation picture of Bang and Hansteen.[22] The method appears to result in relatively simple computations and rather satisfactory agreement with the few available experimental data. However, as pointed out by McGuire,[35] conceptually this extension of the BEA model does not seem to be entirely indisputable. The uncertainty principle does not appear to be satisfied, and also the applied identification procedure for introducing the projectile path, and thus the impact parameter, might seem somewhat artificial. Further work will show whether this most recent extension of the BEA model is well founded and proves to be fruitful.

3.1.3. Semiclassical Approximation (SCA)

The simplicity of the approach of the semiclassical approximation model for atomic Coulomb excitation should be stressed. The motion of the impinging particle in the field of the target nucleus is treated classically, whereas the transition of the inner-shell electron to the continuum is studied quantum mechanically.

The necessary and sufficient condition for a classical treatment of the incoming, ionizing particle is[27b]

$$2Z_1Z_2e^2 \gg \hbar v_1 \tag{14}$$

where, as above, the indices 1 and 2 refer to the projectile and target nucleus, respectively. Provided the condition in Eq. (14) is satisfied, the SCA theory permits calculations of differential as well as total Coulomb ionization cross sections.[22,23]

The treatment of the atomic Coulomb excitaton in the SCA formulation has hitherto been based on first-order time-dependent perturbation theory in impact parameter form and using unperturbed single-electron

wave functions. The Coulomb interaction between the bound inner-shell electron and the bare projectile nucleus is used as the perturbing potential

$$V = \frac{Z_1 e^2}{|\mathbf{r} - \mathbf{R}(t)|} \tag{15}$$

with $\mathbf{R}(t)$ denoting the time-dependent position vector of the electron. By the introduction of hyperbolic paths in Eq. (15) it may be shown that the deflection of the bombarding particle in the Coulomb field of the target nucleus plays an important part in determining the magnitude of the ionization cross sections for low projectile energies.

One further advantage of the SCA model is that for high projectile energies, i.e., projectile paths degenerated into straight lines, the SCA model yields differential Coulomb ionization cross sections $d\sigma/dE_f$ exactly equivalent to the corresponding PWBA expression.[22,37]

The computational difficulties connected with the application of the complete SCA model are very large. The straight-line SCA modification is considerably more manageable and is, at present, in frequent use.[38]

3.1.4. Perturbed Stationary State Approximation

Very recently a formal framework for the theory of atomic inner-shell Coulomb ionizations by heavy charged particles has been given.[39–41] From standard perturbed stationary state theory[42] formulas containing perturbed atomic wave functions have been developed. Atomic wave functions at the distance of closest approach of the projectile are exploited. More specifically, the eigenfunctions used are those of the target atom perturbed by the projectile point charge at rest at the distance of closest approach from the target nucleus. In slow collisions, the approximation of Brandt and co-workers includes two effects not contained in the PWBA. They were originally incorporated into the theory a decade ago by Brandt *et al.*[43] These effects are: (1) an increase in the binding energy felt by the electron to be ejected ("binding effect") in the presence of the moving projectile inside the electron shell in question; (2) the Coulomb deflection of the projectile in the field of the target nucleus, this effect being incorporated in an approximate manner as inspired by the semiclassical model. This approximation has led to close agreement between theory and experiment.[39,41]

For a more detailed discussion of the theories of Coulomb ionization we refer to Hansteen[44] and Madison *et al.*[24] For a comparison with experimental results we refer to Chapter 17 of this book and references therein.

3.2. *Molecular Excitation*

In the course of the discussion of the inner-shell vacancy production mechanisms, we always have to bear in mind that the various methods discussed here are "valid" only for certain regions of Z_1/Z_2 and v_1/u as shown in Figure 4. The Coulomb ionization processes mainly occur in the lower part of this figure. When it became apparent that, for $Z_1 \approx Z_2$ and $v_1 \ll u$, the observed cross sections for inner-shell ionization (at least for small Z) were many orders of magnitude larger than predicted by any approximation discussed so far, Fano and Lichten[45] and Lichten[46] proposed that electron promotion via crossing molecular orbitals (MO) was the reason. This region is shown in Figure 4 (upper left). In this molecular orbital model, vacancies in the higher orbitals of the diatomic quasi-molecule can be filled by electrons from lower orbitals (electron promotion) giving rise to a finite probability that, after collision, the separated atoms have inner-shell vacancies. Lichten[46] and also later Barat and Lichten[47] discuss this process in terms of diabatic correlation diagrams. In Figure 5 we give the best known example of such a diabatic one-electron correlation diagram: the symmetric Ar–Ar collision[46] where, at large internuclear distances, the energy levels are those of Ar, whereas at zero internuclear distance they are those of the united Kr atom. The large decrease in the binding energy of the two $4f_\sigma$ electrons originating from the 2p shell of the separated atoms is the most dominant feature. Saris[48] and Saris and Onderdelinden[49] measured the L-shell, x-ray production cross

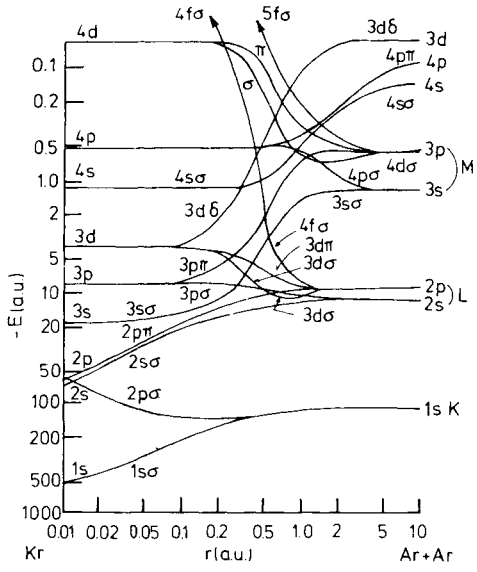

Figure 5. Nonrelativistic correlation diagram of the symmetrical collision Ar plus Ar.

sections in Ne and Ar gas targets for various projectiles from H^+ to Ti^+at bombarding energies below 130 keV. These data clearly show that heavy ions produce x-rays at a rate that is orders of magnitude larger than that predicted by direct Coulomb ionization at these low energies. Similar results were found for K–vacancy production in many low-Z solid targets.[50–51] The enhanced cross sections and the existence of an apparent threshold (connected with the onset of the $4f_\sigma$ promotion) for x-ray production lend support to the MO model of inner-shell ionization.

Because of the large amount of experimental data and their (at least partial) description within this MO model we refer for details to Chapter 17 of this book as well as to several reviews.[52–55]

Because of the complexity of the colliding atoms or ions with their large numbers of electronic levels and transitions involved, an *ab initio* theoretical treatment that is tractable for large systems has not been given so far. Most calculations are done in a two- (few-) level approximation using either an adiabatic or diabatic representation.[55–57] For systems with a few electrons only, and thus very small Z, a full molecular treatment is possible but is out of practical reach for all other collisions. Often the exact number of electrons in the real system is virtually unknown over the full collision path. Evidently, K excitation is the most manageable problem for a quantitative analysis within a one-electron MO diagram model, since the $2p_\sigma$–$2p_\pi$ level crossing is isolated and the states that couple, by rotational interaction, are as near to hydrogenic as one can get. This process has been treated first by Briggs and Macek[58] and Astner *et al.*[59] using a scaled D_2^+ model. Not only do the experimental total cross sections agree well with the theoretical ones near excitation threshold, e.g., up to 300 keV Ne^+–Ne, but so also does the characteristic doubly peaked shape of the cross section as function of the impact parameter,[60] providing a clear distinction from the Coulomb excitation mechanism. But even this K-shell ionization, which is the relatively simplest problem in this connection, is not fully understood. In the schematic correlation Figure 6, we see all possible electronic transitions (a)–(e) that can leave K vacancies in one of the collision partners after the collision.[61] As just discussed, the $2p_\sigma$–$2p_\pi$ electron promotion process (a) via rotational coupling is the most powerful process as long as there are vacancies in the $2p(H)$ state. Generally, this is no longer true for $Z_1, Z_2 > 10$ although in solids such vacancies can be produced in multiple collision processes (see Refs. 10, 24, 26). Also, two-step processes, with long-range radial coupling of the $2p_\pi$ state to suitable vacant atomic orbitals at the beginning of the collision, can produce the vacancies needed to bring process (a) into play. Processes (b) and (c) are the direct excitation processes of the $2p_\sigma$ and the $1s_\sigma$ electrons, respectively, to the continuum and to vacant bound MO's. Also process (e) followed by (a) leads to a $2p_\sigma$ electron hole.

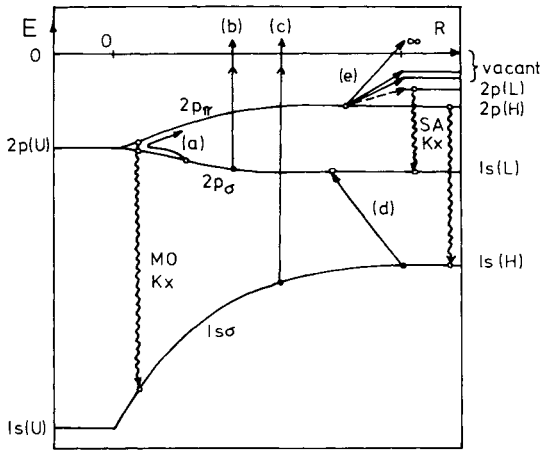

Figure 6. Schematic molecular orbital diagram of the innermost levels for an assymetric collision. *H*, *L*, and *U* refer to the higher-*Z*, lower-*Z*, and united atom, respectively; (a) shows the $2p_\pi$–$2p_\sigma$ level coupling, (b), (c), and (e) are direct ionization processes into vacant bound levels or the continuum, and (d) stands for the vacancy-sharing process of the two lowest levels.

Once formed, a $2p_\sigma$ vacancy can be shared between the $1s(L)$ and $1s(H)$ states. If w is the branching ratio, the cross sections for K-vacancy production in the lower-Z and higher-Z collision partners are given according to Meyerhof[62] by

$$\sigma_K(L) = (1-w)\sigma(2p_\sigma)$$

$$\sigma_K(H) = w\sigma(2p_\sigma) + \sigma(1s_\sigma)$$

where in the absence of direct $2p_\pi$ vacancies as well as multiple collision effects

$$\sigma(2p_\sigma) = \sigma_{(e)-(a)} + \sigma_{(b)}$$

$$\sigma(1s_\sigma) = \sigma_{(c)}$$

The $2p_\sigma \rightarrow 1s(H)$ vacancy transfer probability w has been computed[62] using a schematic radial coupling process first proposed by Nikitin and also examined by Demkov.* Because of the absence of good quantitative single-mechanism cross sections, Meyerhof *et al.*[62] used scaling laws and thus were able to fit the cross sections for the K vacancy productions quite

* For a review of this subject see Ref. 63.

well. This model explains the steep increase in the cross section for the projectile in the vicinity of the near-symmetric collision.

These semitheoretical considerations are far from the point where they could be generalized for all parts of the periodic system where different effects may be more important. It is worth mentioning here that, in very heavy systems, strong relativistic effects come into play and even change the structure of the correlation diagrams so that all scaling procedures fitted to low-Z results become very questionable.

In summary it appears that in special regions inner-shell ionization phenomena are well understood. For $Z_1 \approx Z_2$ and $v_1 \ll u$, the molecular promotion model gives a satisfactory and often a quantitative account of the excitation process. Particularly in medium-Z collision systems, the one-electron $2p_\sigma$–$2p_\pi$ coupling model in combination with the vacancy-sharing concept describes K excitation quite well. For $Z_1 \ll Z_2$ and $v_1 \approx u$, close agreement between theory (e.g., the SCA) and experiment can be obtained, and binding energy effects seem to be fairly well under control. Excitation of higher than K shells still gives some problems, probably due to uncertainties in the interatomic potential and the wave functions. For $v_1 > u$, little experimental data exist since the ion energies involved in inner-shell excitation are quite high in this relative velocity scheme. For increasing Z_1, a simple Z_1^2 scaling soon becomes insufficient, and other effects, such as charge exchange, grow in (as yet not quantified) importance.

The region between Coulomb excitation and molecular excitation is still a no-man's land. Experiments are scarce and a satisfactory theory does not exist. It is safe to predict that interesting things are going to happen here.

4. *United Atom Phenomena and Related Processes*

4.1. *Molecular Orbital (MO)X-Rays; REC*

A most interesting phenomenon is observed during heavy ion collisions. If a vacancy in an inner molecular level decays during the collision a quasimolecular noncharacteristic x-ray or MO x-ray can be observed. This process is schematically introduced in Figure 6, where a $2p_\sigma$–$1s_\sigma$ (usually called MO K x-ray) transition is shown. A very rough estimate of the probability of such a process is given by t_1/τ_K, where t_1 is the collision time and τ_K the K-vacancy lifetime. For 30-MeV Br–Br this ratio is of the order of 10^{-16} sec/10^{-13} sec $\approx 10^{-3}$. For L and M vacancy decay this number can be of the order of 10^{-1}.

The pioneering experiment in this field was made in 1934 by Coates,[64] who measured the x-ray production cross section for several

targets after the bombardment with 2.4-MeV mercury ions. To explain his observed large cross sections he proposed that the ionization mechanism is one of the time-varying molecular interactions rather than a direct Coulomb interaction. He also observed that some x-rays were not characteristic of either the beam or the target. These two important observations were, unfortunately, ignored for some 30 years.

The first experimental evidence and interpretation for MO L x-rays was found by Saris *et al.*[65] in Ar–Ar collisions in 1971 without knowledge of the experiments of Coates. Molecular orbital M x-rays were found by Mokler *et al.*[66] in I collisions with Au, Th, and U, and MO K x-rays were first detected by McDonald *et al.*[67] in C–C collisions. Meanwhile many other groups have reported the detection of several MO x-rays. A summary may be found in Refs. 68 and 69.

The observed spectra may be divided into two groups. The K MO x-rays show a continuum spectrum, whereas the M (and some L) MO spectra have a definite peak structure or at least shoulder behavior.

If a vacancy is present in a molecular level the transition can take place at any value of the internuclear distance R with the probability proportional to the time spent around a distance R and proportional to the multipole transition probability integrated over all possible Rutherford trajectories. For the K x-ray electronic transition the transition energy is a continuous function of the internuclear distance R. Hence the MO K x-ray spectrum is a continuum extending above the united atom limit because the collision is a dynamic process connected to the lifetime of the vacancy, the finite collision time, and the time dependence of the MO energy levels. Much effort has been put into the interpretation of these spectra, especially by the group of Greiner *et al.*,[70] as well as Meyerhof.[71]

A quantity that is discussed and measured nowadays by many groups is the anisotropy of the emitted radiation. This is a quantity where details of the sublevel occupation probabilities as well as the behavior of the wave functions and their variations with time at small internuclear distances come into effect. Details of this interesting field may be found in Refs. 69, 72, and 73.

A very simple quasistatic interpretation for MO M x-rays for the colliding I–Au system is given by Fricke *et al.*[74] They have calculated in a self-consistent way the correlation diagram of this system making use of the relativistic Hartree–Fock–Slater method so that all relativistic effects, spin–orbit splitting as well as the screening, are fully taken into account. From this correlation diagram they have extracted all possible transitions within the energy range of 5–11 keV, where the experimental MO M peak occurs. After exact integration over all possible Rutherford trajectories using dipole transition probabilities and a collision broadening of 0.5 keV, they obtain the spectrum (b) in Figure 7, where (a) is the observed spec-

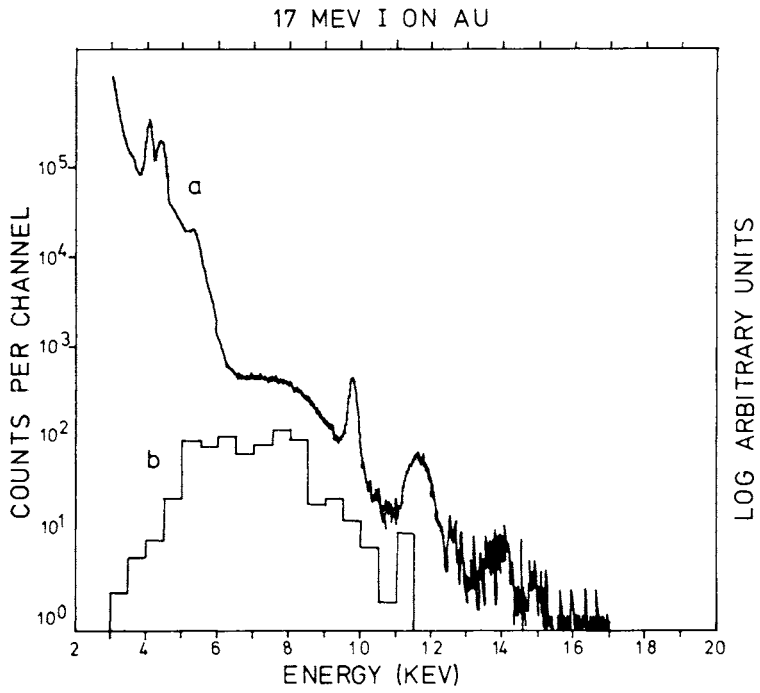

Figure 7. (a) Experimental spectrum of 17-MeV I on Au corrected for absorber; (b) calculated spectrum using a realistic Dirac–Fock–Slater correlation diagram[74] which reproduces the MO peak at 8 keV rather well.

trum. Using this method the correct structure and behavior is fairly well reproduced. A similar interpretation[75] for the L MO x-rays of the system I–Ag showed equally good results.

Since coincidence spectra as functions of the scattering angle of the colliding atom have begun to be available,[76] the experimental observations and theoretical interpretations of the molecular orbital x-rays have come into a second, even more interesting phase. The impression after the first five years of investigation of these noncharacteristic x-rays is that a basic interpretation can be given but that most details need further investigation.

During the course of these investigations another effect, long expected from astrophysicists, has been found by Schnopper *et al.*[77]: radiative electron capture (REC). This is the radiative capture into vacant projectile states of loosely bound target electrons. In such a transition, the normal transition energy of the bound atomic state is added to the energy of motion of the electron relative to the projectile. This makes the peak shift with varying projectile energy and also with the scalar product of the

momentum of the projectile and the electron wave function, thus making it possible to extract important information on the momentum distribution of the electron from the detailed investigation of the shape of the REC peak.[78] More details, as well as information, on effects like radiative Auger effect (RAE), radiative electron rearrangement (RER) or radiative ionization (RI) may be found by K.-H. Schartner in Chapter 17 of this work.

For the discussion of the electron bremsstrahlung and nuclear bremsstrahlung, which may also become important in the analysis of the spectra, we can only refer to Refs. 71, 79, and 80.

4.2. Positron Emission in U–U Collision

If we go back to Figure 3, where we have considered the atomic behavior of atoms with $Z > 100$, we can see that at or about $Z \approx 173$ the $1s$ level reaches the negative continuum of electrons. At that point this discussion seemed to become purely academic.

Now in view of the MO x-rays and possible positron emission in U–U collisions these values become most important even for the experimentalists. The values in Figure 3 are then united atom collision limits of very heavy atoms and are usually drawn on the left-hand side of the correlation diagrams (see Figure 5).

In the MO M x-rays observed by Mokler *et al.*,[66] information from quasiatoms with $Z_1 + Z_2$ up to 145 can already be obtained. Proceeding to even heavier colliding systems, at some point a limit is reached where the lowest level dives into the negative continuum. Müller *et al.*[70] have examined the physics of this process and found that nothing observable happens as long as a full $1s$ shell reaches the continuum. But if the $1s$ shell carries a vacancy down into the negative continuum it is possible that an electron from the negative continuum occupies this level thus leaving a hole in the continuum. This hole is a positron, which will be emitted immediately and may be observed. Greiner and co-workers[81] calculated the spectrum of the emitted positrons as a function of the projectile and target Z as well as their incident energy. Because a positron is easy to detect this experiment using the U – U, or even better the U – Cf, collision seems to be the easiest way to get information from a region where QED effects are most important.

In various respects the dynamics of the collision process not discussed so far play a most dominant role in the discussion of the positron experiment.* First, the dynamical broadening of the energy levels may already

* The experiment is well underway; first results were already presented at GSI Seminars 1977; see Ref. 82.

create a electron–positron pair before the adiabatic level reaches the negative continuum. Second, it is shown by first simplied coupled-channel calculations[83,84] that for small impact parameters there is a chance on the order of a few percent of direct vacancy formation in the $1s$ level during the collision. Third, there is a large probability of direct (Coulomb) formation[85] of electron–positron pairs in the time-varying field of the quasisuperheavy molecule as well as a secondary product following Coulomb ionization[86] of the nucleus.

In conclusion one may predict that the whole field of inner shells briefly discussed in this chapter will be one of the most interesting fields in the future of modern atomic physics.

Acknowledgments

To Professor J. M. Hansteen at Bergen, I am highly indebted for his contribution of the Coulomb ionization processes. I gratefully acknowledge very stimulating comments and discussions with many colleagues engaged in the physics of inner shells as well as partial financial support from Gesellschaft für Schwerionenforschung (GSI).

References

1. D. R. Hartree, *Proc. Cambridge Phil. Soc.* **24**, 89 (1927); V. Fock, *Z. Phys.* **61**, 126 (1930); **62**, 795 (1930).
2. P. A. M. Dirac, *Proc. R. Soc. London* **117**, 610 (1928); **118**, 351 (1928).
3. I. P. Grant, *Adv. Phys.* **19**, 747 (1970); F. P. Larkins, in *Atomic Inner Shell Processes*, Ed. B. Craseman, p. 377, Academic Press, New York (1975); I. Lindgren and A. Rosén, *Case Stud. At. Phys.* **4**, 93 (1974).
4. R. D. Cowan, *Phys. Rev.* **163**, 54 (1967).
5. G. Breit, *Phys. Rev.* **35**, 1447 (1930); **37**, 51 (1931); Y. K. Kim, *Phys. Rev.* **154**, 17 (1967); J.-P. Desclaux, Thèse, Université de Paris (1971).
6. J. Schwinger, *Phys. Rev.* **75**, 651 (1949); B. Fricke, *Z. Phys.* **218**, 495 (1969).
7. G. E. Brown, J. S. Langer, and G. W. Schaefer, *Proc. R. Soc.* **A251**, 92 (1959); G. E. Brown and D. F. Mayers, *Proc. R. Soc.* **A251**, 105 (1959).
8. A. M. Desiderio and W. R. Johnson, *Phys. Rev. A* **3**, 1267 (1971).
9. P. J. Mohr, *Ann. Phys. N.Y.* **88**, 26 (1974); **88**, 52 (1974).
10. J. D. Garcia, R. J. Fortner, and T. M. Kavanagh, *Rev. Mod. Phys.* **45**, 111 (1973).
11. N. Stolterfoht, in *Proceedings of the Eighth International Conference on the Physics of Electronic and Atomic Collisions*, Belgrade, Invited papers, Eds. B. C. Cobic and M. V. Kurepa, p. 117 (1974); papers in *Electronic and Atomic Collisions*, Eds. J. S. Risley and R. Geballe, University of Wash. Press, Seattle (1975).

12. P. Ziem, R. Bruch, and N. Stolterfoht, *J. Phys.* **B8**, L480 (1975); N. Stolterfoht and U. Leithäuser, *Phys. Rev. Lett.* **36**, 186 (1976); K. O. Groeneveld, G. Nolte, S. Schumann, and K. D. Sevier, *Phys. Lett.* **56A**, 29 (1976); R. Bruch, G. Paul, J. Andrä, and B. Fricke, *Phys. Lett.* **53A**, 293 (1975).
13. S. Schumann, K.-O. Groeneveld, and K. D. Sevier, *Abstracts of Contributed Papers of the Fifth International Conference on Atomic Physics*, Eds. R. Marrus and M. Prior, p. 191, Berkeley, July 1976.
14. J. Raefelski, B. Fulcher, and W. Greiner, *Nuovo. Comento* **13B**, 135 (1973).
15. B. Fricke, J.-P. Desclaux, and J. T. Waber, *Phys. Rev. Lett.* **28**, 714 (1972).
16. F. T. Porter and M. S. Freedman, *Phys. Rev. Lett.* **27**, 293 (1971).
17. G. L. Borchert, *Z. Naturforsch.* **31a**, 102 (1974); G. L. Borchert and B. Fricke, *Abstracts of Contributed Papers to the Fifth International Conference on Atomic Physics*, Ed. R. Marrus and M. Prior, p. 321, Berkeley, July 1976.
18. B. Fricke and G. Soff, Gesellschaft für Schwerionenforschung report No. GSI-T1-74 (1974).
19. B. Fricke and J. T. Webaber, *Actin. Rev.* **1**, 433 (1971); B. Fricke, *Struct. Bonding* (Berlin) **21**, 89 (1975); B. Fricke, *Naturwissenschaft* **63**, 162 (1976).
20. B. Müller, J. Rafelski, and W. Greiner, *Z. Phys.* **257**, 82 (1972); **257**, 163 (1972).
21. E. Merzbacher and H. W. Lewis, in *Handbuch der Physik*, Vol. **34**, p. 166, Ed. S. Flügge, Springer-Verlag, Heidelberg (1958).
22. J. Bang and J. M. Hansteen, *Mat. Fys. Medd. Dan. Vid. Selsk.* **31**, No. 13 (1959).
23. J. M. Hansteen and O. P. Mosebekk, *Nucl. Phys.* **A201**, 541 (1973).
24. D. H. Madison and E. Merzbacher, in *Atomic Inner Shell Processes*, Ed. B. Craseman, p. 1, Academic Press, New York (1975).
25. Q. C. Kessel and B. Fastrup, *Case Stud. At. Phys.* **3**, 137 (1973).
26. H. A. Bethe, *Ann. Phys. (Leipzig)*, **5**, 325 (1930).
27. (a) E. J. Williams, *Rev. Mod. Phys.* **17**, 217 (1945); (b) N. Bohr, *Kl. Dan. Vidensk. Selsk. Mat.-Fys. Medd.* **18**, No. 8 (1948).
28. W. Henneberg, *Z. Phys.* **86**, 592 (1933); G. S. Khandelwal, B. H. Choi, and E. Merzbacher, *At. Data* **1**, 103 (1969); B. H. Choi, E. Merzbacher, and G. S. Khandelwal, *At. Data* **5**, 291 (1973).
29. C. H. Rutledge and R. L. Watson, *At. Data Nucl. Data Tables* **12**, 195 (1973).
30. D. Jamnik and C. Zupancic, *Kl. Dan. Vidensk. Selsk. Mat.-Fys. Medd.* **31**, No. 2 (1957).
31. J. D. Garcia, *Phys. Rev. A* **1**, 280 1402 (1970).
32. M. Gryzinski, *Phys. Rev.* **A138**, 336 (1965).
33. L. Vriens, *Case Stud. At. Phys.* **1**, 335 (1969).
34. J. S. Hansen, *Phys. Rev. A* **8**, 822 (1973).
35. J. H. McGuire, *Phys. Rev. A* **9**, 286 (1974).
36. J. H. McGuire and K. Omidvar, *Phys. Rev. A* **10**, 182 (1974).
37. H. A. Bethe and R. W. Jackiw, in *Intermediate Quantum Mechanics*, 2nd ed., Benjamin, New York (1968).
38. J. M. Hansteen, O. M. Johnson, and L. Kocbach, *J. Phys.* **B7**, L271 (1974), and references quoted therein.
39. G. Basbas, W. Brandt, and R. Laubert, *Phys. Rev. A* **7**, 983 (1973).
40. G. Basbas, W. Brandt, and R. H. Ritchi, *Phys. Rev. A* **7**, 1971 (1973).
41. W. Brandt and G. Lapicki, *Phys. Rev. A* **10**, 474 (1974).
42. N. F. Mott and H. S. W. Massey, *The Theory of Atomic Collisions*, 3rd ed., Oxford University Press, London (1965).
43. W. Brandt, R. Laubert, and I. Sellin, *Phys. Rev.* **151**, 56 (1966).
44. J. M. Hansteen, *Adv. At. Mol. Phys.* **11**, 299 (1975).
45. U. Fano and W. Lichten, *Phys. Rev. Lett.* **14**, 627 (1965).
46. W. Lichten, *Phys. Rev.* **164**, 131 (1967).

47. M. Barat and W. Lichten, *Phys. Rev. A* **6**, 211 (1972).
48. F. W. Saris, *Physica* **52**, 290 (1971).
49. F. W. Saris and D. Onderdelinden, *Physica* **49**, 441 (1970).
50. W. Brandt and R. Laubert, *Phys. Rev. Lett.* **24**, 1037 (1970).
51. R. C. Der, R. J. Fortner, T. M. Kavanagh, and J. M. Khan, *Phys. Rev. A* **4**, 556 (1971); M. Terasawa, T. Tamura, and H. Kamada *Abstracts of the Proceedings of the Seventh International Conference on the Physics of Electronic and Atomic Collisions*, Amsterdam, p. 410, North-Holland, Amsterdam (1970).
52. *Atomic Physics* 4, Eds. G. zu Putlitz, E. W. Weber, and A. Winnacker, Plenum Press, New York (1975).
53. W. Lichten, p. 249 of Ref. 52.
54. P. Richard, in *Atomic Inner Shell Processes*, Ed. B. Craseman, p. 73, Academic Press, New York (1975).
55. J. S. Briggs, Invited Talk, *Ninth International Conference on the Physics of Electronic and Atomic Collisions*, University of Washington, Seattle, July 1975.
56. F. T. Smith, *Phys. Rev.* **179**, 111 (1969); F. T. O'Malley, *Adv. At. Mol. Phys.* **7**, 223 (1971).
57. V. Sidis and H. Lefebvre-Brion, *J. Phys.* **B4**, 1040 (1971).
58. J. S. Briggs and J. Macek, *J. Phys.* **B5**, 579 (1972).
59. G. Astner, J. D. Garcia, and L. Liljeby, *J. Phys.* **B8**, L314 (1975).
60. G. Sackmann, H.-O. Lutz, and J. S. Briggs, *Phys. Rev. Lett.* **32**, 805 (1974); KFA report No. Jül-1154-KP (1975).
61. W. E. Meyerhof, "International Seminar on Ion-Atomic Collisions," Gif-sur-Yvette, France, July 1973; W. E. Meyerhof, *Comm. Atom. Mol. Phys.* **5**, 33 (1975).
62. W. E. Meyerhof, *Phys. Rev. Lett.* **31**, 1341 (1973); J. S. Briggs and K. Tjaulberg, *J. Phys.* **B8**, 1909 (1975).
63. E. E. Nikitin, *Adv. Quantum Chem.* **5**, 135 (1970).
64. W. M. Coates, *Phys. Rev.* **46**, 542 (1934).
65. F. W. Saris, W. F. van der Weg, H. Tavara, and R. Laubert, *Phys. Rev. Lett.* **28**, 717 (1972).
66. P. H. Mokler, H.-J. Stein, and P. Armbruster, *Phys. Rev. Lett.* **29**, 827 (1972).
67. J. R. McDonald, M. D. Brown, and T. Chiao, *Phys. Rev. Lett.* **30**, 471 (1973).
68. F. W. Saris and F. J. de Heer, p. 287 of Ref. 52; F. W. Saris and Th. Hoogkamer, in *Atomic Physics* 5, Eds. R. Marrus, M. Prior, and H. Shugort, Plenum Press, New York (1977).
69. P. H. Mokler, S. Hagmann, P. Armbruster, G. Kraft, H.-J. Stein, K. Rashid, and B. Fricke, p. 301 of Ref. 52.
70. B. Müller, R. K. Smith, and W. Greiner, p. 209 of Ref. 52, and references therein; B. Müller, in *Invited Lectures Review Papers and Progress Reports of the Ninth International Conference on the Physics of Electronic and Atomic Collisions*, Eds. J. S. Risley and R. Geballe, p. 481, University of Washington Press, Seattle (1976).
71. W. E. Meyerhof, T. K. Saylor, S. M. Lazarus, A. Little, B. B. Triplett, L. F. Chase, and R. Anholt, *Phys. Rev. Lett.* **32**, 1279 (1974).
72. *Abstracts of Contributed Papers, Second International Conference Inner Shell Ionization Phenomena*, Eds. W. Melhorn and R. Brenn, Freiburg University Press, Freiburg, March 1976.
73. Ch. Stoller, p. 1 of Ref. 72, and references therein.
74. B. Fricke, T. Morović, W.-D. Sepp, A. Rosén, and D. E. Ellis, *Phys. Lett.* **59A**, 375 (1976).
75. T. Morović, B. Fricke, W.-D. Sepp, A. Rosén, and D. E. Ellis, *Phys. Lett.*, **63A**, 12 (1977).
76. I. Tseruja, H. Schmidt-Böcking, R. Schulé, R. Schuch, H. Bethge, and H.-J. Specht, p. 9 of Ref. 72.

77. H. W. Schnopper, H.-D. Betz, J.-P. Delvaille, K. Kalata, A. R. Sohval, K. W. Jones, and H. E. Wegner, *Phys. Rev. Lett.* **29**, 898 (1972); P. Kienle, M. Kleber, B. Povh, R. M. Diamond, F. S. Stephens, E. Grosse, M. R. Maier, and D. Proetel, *Phys. Rev. Lett.* **31**, 1099 (1973).
78. M. Kleber and D. H. Jakubassa, *Nucl. Phys.* **A252**, 152 (1975), and references therein.
79. J. S. Greenberg, C. K. Davis, and P. Vincent, *Phys. Rev. Lett.* **32**, 1215 (1974).
80. D. H. Jakubassa and M. Kleber, *Z. Phys.* **A273**, 29 (1975).
81. H. Peitz, B. Müller, J. Rafelski, and W. Greiner, *Lett. Nuovo* Cimento **8**, 37 (1973); K. Smith, H. Peitz, B. Müller, and W. Greiner, *Phys. Rev. Lett.* **32**, 554 (1974); and Ref. 70.
82. R. Backe *et al.*, GSI Seminars 1977 (to be published).
83. D.-H. Jakubassa, *Phys. Lett.* **58A**, 163 (1976).
84. W. Betz, G. Soff, B. Müller, and W. Greiner, *Phys. Rev. Lett.* **37**, 1046 (1976).
85. G. Soff, J. Reinhardt, B. Müller, and W. Greiner, *Phys. Rev. Lett.* **38**, 592 (1977).
86. V. Oberacker, G. Soff, and W. Greiner, *Phys. Rev. Lett.* **36**, 1024 (1976).